Egyptian Journal of Petroleum (2016) xxx, xxx–xxx

HOSTED BY

ELSEVIER

Egyptian Petroleum Research Institute

Egyptian Journal of Petroleum

www.elsevier.com/locate/egyjp
www.sciencedirect.com

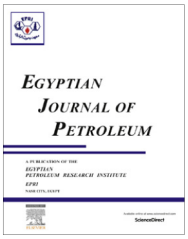

FULL LENGTH ARTICLE

# Synthesis of non-ionic surfactants based on alkylene diamine and evaluation of their corrosion inhibition efficiency on carbon steel in formation water

**A.M. Al-Sabagh, N.M. Nasser, E.A. Khamis, Tahany Mahmoud** *

*Egyptian Petroleum Research Institute (EPRI), Nasr City, Cairo, Egypt*

Received 22 December 2015; revised 12 February 2016; accepted 6 March 2016

**KEYWORDS**

Potentiodynamic polarization;
Quantum calculations;
Inhibition efficiency;
Formation water

**Abstract** The inhibitive effects of newly synthesized non-ionic surfactant based on alkylene diamine surfactants on X-65 carbon steel in formation water was investigated by means of electrochemical techniques and quantum chemical study. These derivatives were characterized by FT-IR, and the surface tension and thermodynamic parameters were calculated. The polarization showed that the inhibition efficiency of the prepared compounds was increased with increasing the length of the internal alkyl chain between the two terminal amino groups of diamine. The electronic properties obtained using quantum chemical approach were correlated with the experimental inhibition efficiencies. The surface morphology of carbon steel was investigated using SEM.



## 1. Introduction

Carbon steel has been widely employed as construction materials for pipe work in the oil and gas production such as down hole tubular, piping systems and transmission pipelines [1]. Corrosion in the oil field appears as leak in tanks, casing, tubing, pipeline and other equipment. This process changes the base metal to another type of materials. The most corrosive environment in oil field operations is caused by trace amounts of oxygen entering into a sour brine system, as well as the large amounts of carbon dioxide and hydrogen sulfide present in a deep oil well water (formation water) [2]. This type of corrosion forms a scale which varies from dense and adherent to loose, porous and thick [3]. Corrosion inhibitors (mainly, surfactants) are widely employed in the petroleum industry to protect iron and steel equipment used in drilling, production, transport and refining of hydrocarbons [4,5]. The efficiency of the inhibition film depends on the inhibitor concentration and contact time with the metal surface. In fact, introducing of ethylene oxides into surfactant molecule (ethoxylation) increases the inhibiting effect of surfactant [6]. The presence of these groups increases the solubility of surfactant and hence the extent of its adsorption on the metal surface increases and consequently its inhibitive action improves. Many studies on the inhibition of the corrosion of carbon steel by some ethoxylated surfactants have been carried out in different corrosive environments [7–11]. Quantum chemical methods have already proven to be very useful in determining the molecular structure

* Corresponding author.

Peer review under responsibility of Egyptian Petroleum Research Institute.

http://dx.doi.org/10.1016/j.ejpe.2016.03.001



Please cite this article in press as: A.M. Al-Sabagh et al., Synthesis of non-ionic surfactants based on alkylene diamine and evaluation of their corrosion inhibition efficiency on carbon steel in formation water, Egypt. J. Petrol. (2016), http://dx.doi.org/10.1016/j.ejpe.2016.03.001

**Table 1** Chemical Composition of Carbon Steel alloy in wt%.

| Element | C | Mn | Si | S | P | Cr | Ni | V | Al | Mo | Cu | Fe |
|---|---|---|---|---|---|---|---|---|---|---|---|---|
| Content (wt%) | 0.09 | 1.52 | 0.22 | 0.05 | 0.01 | 0.02 | 0.04 | 0.002 | 0.04 | 0.004 | 0.02 | Rest |

**Table 2** Chemical composition and physical properties of deep oil wells formation water used in this investigation.

| Property | Value |
|---|---|
| Density (g/cm$^3$) | 1.044 |
| Turbidity (FAU) | 263 |
| PH | 6.38 |
| Salinity as NaCl (mg/l) | 120.29 |
| **Ionic species** | **Value** |
| Sulfate | 6.5 (mg/l) |
| Phosphate | 0.771 (mg/l) |
| Bi-carbonate | 143 (mg/l) |
| Chloride | 7300 (mg/l) |
| Vanadium as $V_2O_5$ | 450 (μg/l) |
| Iron ferrous | 23 (mg/l) |
| Iron, total | 42 (mg/l) |
| Calcium | 800 (mg/l) |
| Magnesium | 364 (mg/l) |
| Barium | 105 (mg/l) |
| Potassium | 250 (mg/l) |
| Zinc | 1.359 (mg/l) |

as well as elucidating the electronic structure and reactivity [12]. Thus, it has become a common practice to carry out quantum chemical calculations in corrosion inhibition studies. The concept of assessing the efficiency of a corrosion inhibitor with the help of computational chemistry is to search for compounds with desired properties using chemical intuition and experience into a mathematically quantified and computerized form. Once a correlation between the structure and activity or property is found, any number of compounds, including those not yet synthesized, can be readily screened employing computational methodology [13] and a set of mathematical equations which are capable of representing accurately the chemical phenomenon under study [14,15]. The study of corrosion processes and their inhibition by organic inhibitors is a very active field of research [16]. Many researchers report that the inhibitory effect mainly depends on some physicochemical and electronic properties of the organic inhibitor, which relate to its functional groups, steric effects, electronic density of donor atoms, and orbital character of donating electrons, and so on [17,18]. The inhibiting mechanism is generally explained by the formation of a physical and/or chemically adsorbed film on the metal surface [19,20]. This work aims to synthesis new ethoxylated non-ionic surfactants based on 1,4 diaminobutane, 1,6 diaminohexane and 1,8 diaminooctane. The work should be extended to evaluate them as corrosion inhibitors for carbon steel pipelines in deep oil wells formation water. The HOMO and LUMO calculations were used to evaluate the corrosion inhibition efficiency of these surfactants in the light helping of computational chemistry to the practical finding by potentiodynamic techniques.

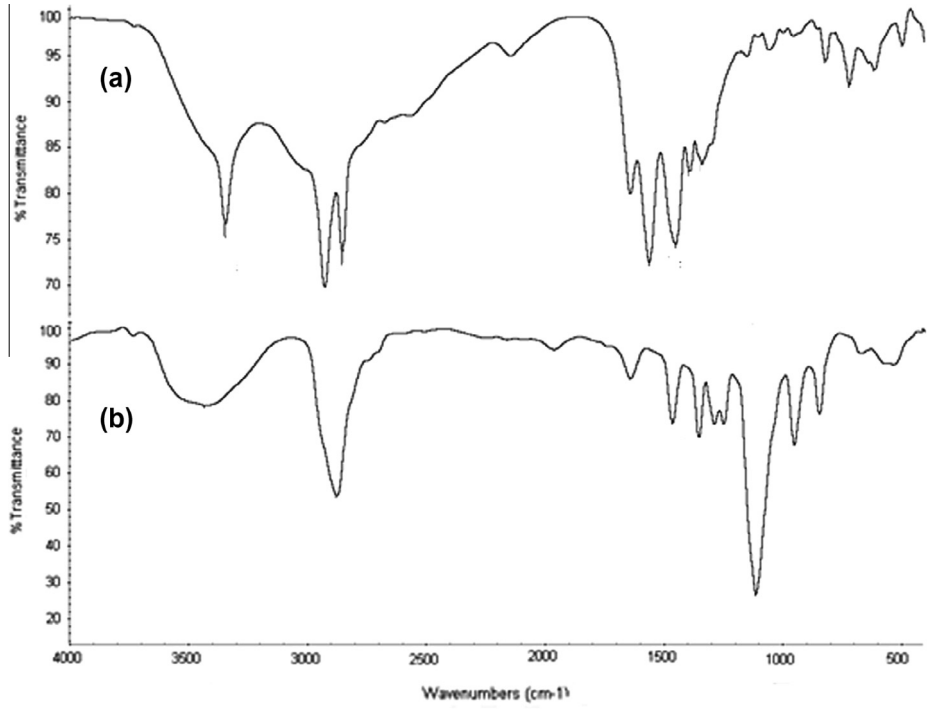


**Figure 1** FTIR spectra for (a) pure 1,8 diaminoctane, (b) ethoxylated 1,8 diaminoctane.

**Table 3** Surface active and thermodynamic properties of DAB, $DAH_{100}$ and $DAO_{100}$ at 25 °C different ratios of ethylene oxide at room temperature.

| Surfactants | Temp. | CMC mole/dm$^3$ | $\gamma_{cmc}$, mN/m | $\Gamma_{max}$, mol/m$^2$ | $A_{min}$, nm$^2$ | $\Pi_{CMC}$ | $\Delta G_{mic}$, kJ/mol | $\Delta G_{ads}$, kJ/mol |
|---|---|---|---|---|---|---|---|---|
| $DABE_{100}$ | 25 °C | $5 \times 10^{-4}$ | 47 | $1.032 \times 10^{-10}$ | 149.3 | 25.3 | −19.1 | −21.59 |
| $DAHE_{100}$ | 25 °C | $3.22 \times 10^{-4}$ | 44 | $1.11 \times 10^{-10}$ | 160.8 | 28.3 | −20.9 | −23.4 |
| $DAOE_{100}$ | 25 °C | $3.0 \times 10^{-4}$ | 41 | $9.28 \times 10^{-11}$ | 178.7 | 31.3 | −22.7 | −26.11 |

## 2. Experimental and techniques

### 2.1. Materials

The working electrode is prepared from a cylindrical carbon steel bar of composition presented in Table 1. The electrode is inserted in a Teflon tube and isolated with epoxy so that only its cross-sectional area (0.5 cm$^2$) is allowed to contact the aggressive solutions. The electrode is polished using different grades of emery paper (600, 800 and 1200) before each experiment, and then rinsed with triply distilled water and finally degreased with acetone.

### 2.2. Deep oil wells formation water

Deepest oil wells formation water naturally exists in the reservoir rocks before drilling. Most oil field water contains a variety of dissolved organic and inorganic compounds. The major species usually present are sodium, calcium, magnesium, chloride, bicarbonate, and sulfate. The chemical composition of the oil wells formation water used in this investigation and its physical properties is shown in Table 2.

### 2.3. Synthesis of the inhibitors

In a 250 ml four-neck flask equipped with a condenser, magnetic stirrer, thermometer, ethylene oxide gas inlet and outlet nozzles. Then Na-metal was added to 1 mol of 1,4-diaminobutane (DAB) or 1,6-diaminohexane (DAH) or (1,8-diaminoctane (DAB)) with stirring at 150–160 °C for about 15 min. Individually, then the ethylene oxide gas was allowed to pass over each compound. The temperature was raised gradually up to reflux temperature and then the reaction mixture was continuously proceeding for 3 h. After that, the mixture was cooled. The progress of the reaction was evaluated by monitoring the gained weight because of insertion of ethylene oxide units. The synthesized structures were identified

**Table 4** Electrochemical polarization parameters for the corrosion of carbon steel in formation water containing various concentrations of the investigated inhibitors.

| Inhibitor blank | Concentration, ppm | $-E_{corr}$, mV vs. SCE | $I_{corr}$, mA cm$^{-2}$ | $\beta_a$, mV dec$^{-1}$ | $-\beta_c$, mV dec$^{-1}$ | $\eta_p$, % |
|---|---|---|---|---|---|---|
| | 0 | 940.8 | 103.0 | 800.1 | 202 | |
| DABE100 | 25 | 856 | 16.41 | 303.3 | 163.3 | 84.1 |
| | 50 | 835.8 | 15.85 | 253.2 | 168.3 | 84.6 |
| | 75 | 851 | 15.03 | 252 | 152.1 | 85.4 |
| | 100 | 838.2 | 14.52 | 222.2 | 182.8 | 85.9 |
| | 125 | 819.2 | 12.12 | 199.2 | 168.2 | 88.2 |
| DAHE100 | 25 | 861.7 | 24.61 | 377.1 | 164.5 | 76.1 |
| | 50 | 860.6 | 20.786 | 270.6 | 172.9 | 79.8 |
| | 75 | 859.6 | 17.10 | 307.9 | 172.9 | 83.4 |
| | 100 | 838.9 | 14.68 | 191 | 163.9 | 85.7 |
| | 125 | 829.4 | 13.46 | 234.6 | 179.2 | 86.9 |
| DAOE100 | 25 | 858.2 | 38.72 | 318.7 | 183.8 | 62.4 |
| | 50 | 825.7 | 27.017 | 188.6 | 163.8 | 73.8 |
| | 75 | 849.8 | 24.212 | 205.3 | 161.2 | 76.5 |
| | 100 | 824.2 | 23.113 | 256.6 | 173.5 | 77.6 |
| | 125 | 810.3 | 16.6 | 163.4 | 133.8 | 83.9 |
| DAOE50 | 25 | 883.5 | 45.395 | 416.2 | 173.9 | 55.9 |
| | 50 | 876.6 | 27.127 | 323.3 | 161.6 | 73.7 |
| | 75 | 857.2 | 25.457 | 256 | 179.4 | 75.3 |
| | 100 | 844.2 | 24.099 | 214.1 | 147.7 | 76.6 |
| | 125 | 830 | 21.126 | 239.4 | 163.3 | 79.5 |
| DAOE150 | 25 | 904.6 | 31.419 | 257.5 | 144.1 | 69.4 |
| | 50 | 895.8 | 23.826 | 254.7 | 157.2 | 76.8 |
| | 75 | 864.7 | 21.82 | 243.2 | 177.5 | 78.8 |
| | 100 | 852.6 | 18.54 | 170.5 | 175.6 | 82 |
| | 125 | 840.3 | 15.049 | 122.6 | 182.9 | 85.3 |

Please cite this article in press as: A.M. Al-Sabagh et al., Synthesis of non-ionic surfactants based on alkylene diamine and evaluation of their corrosion inhibition efficiency on carbon steel in formation water, Egypt. J. Petrol. (2016), http://dx.doi.org/10.1016/j.ejpe.2016.03.001

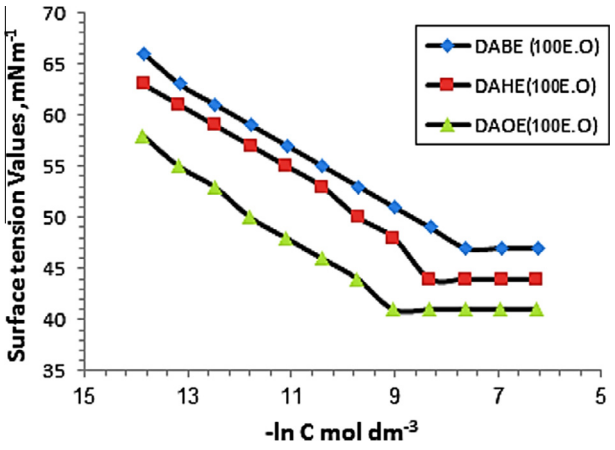


**Figure 2** Surface tension vs. ln C of the three surfactants [$DABE_{100}$, $DAHE_{100}$, $DAOE_{100}$] at room temperature.

by IR spectroscopic analyses. The FTIR spectrum of the purified (dried) and ethoxylated samples is shown in Fig. 1(a and b) for the 1,8 diaminooctane as representative samples, and it shows that stretching band at 3400 $cm^{-1}$ for $NH_2$ and OH group. The characteristic band for the ethoxylation appeared at 1104 $cm^{-1}$. The stretching bands at 2923 and 2854 $cm^{-1}$ are denoted to $CH_2$ of the alkylene group.

### 2.4. Surface tension measurements ($\gamma$)

The surface tension ($\gamma$) was measured using (Kruss K6 Tensiometer type, a direct surface tension measurement using the ring method) for various concentrations of the investigated surfactants.

### 2.5. Potentiodynamic polarization measurements

The electrochemical measurements were carried out using Volta lab80 (Tacussel-radiometer PGZ402) controlled by Tacussel corrosion analysis software model (Volta master 4). A platinum electrode was used as auxiliary electrode. All potentials were measured against a saturated calomel electrode (SCE) as a reference electrode. All the measurements were carried out in air-saturated solutions and at ambient temperature (298 K).

### 2.6. Quantum chemical study

The molecular structures of the inhibitors undertaken have been fully geometrically optimized via single point ab initio method (3-21G basis set) using Austin model 1 (AM1) with Hyperchem quantum chemistry software [21]. The quantum chemical parameters calculated are the energy of the highest occupied molecular orbital ($E_{HOMO}$, eV), the energy of the lowest unoccupied molecular orbital ($E_{LUMO}$, eV), the energy gap ($\Delta E = E_{LUMO} - E_{HOMO}$, eV) and the dipole moment ($\mu$, debye) [22].

## 3. Results and discussion

### 3.1. Chemical structure effect

The inhibition efficiency of the organic compounds depends on many factors, including the number of adsorption sites and their charge density, molecular size, heat of hydrogenation, mode of interaction with the metal surface and formation of metallic complexes [23]. The studied original compounds contain the same number of nitrogen atoms (2 atoms attached to the molecule) but they differ only in the internal alkyl chains (No. of carbon atoms). These three starting amines are ethoxylated individually with 100 units from ethylene oxide to yield the ethoxylated products $DAOE_{100}$, $DAHE_{100}$ and $DABE_{100}$. Therefore, the difference between them is the number of internal alkyl chains. This difference is the reason for the good adsorption of ethoxylated 1,4 diaminobutane ($DABE_{100}$) than ($DAHE_{100}$ and $DAOE_{100}$).

On the other hand, for the different ethylene oxide number applied on 1,8 diaminooctane, it was found that $DAOE_{150}$ is

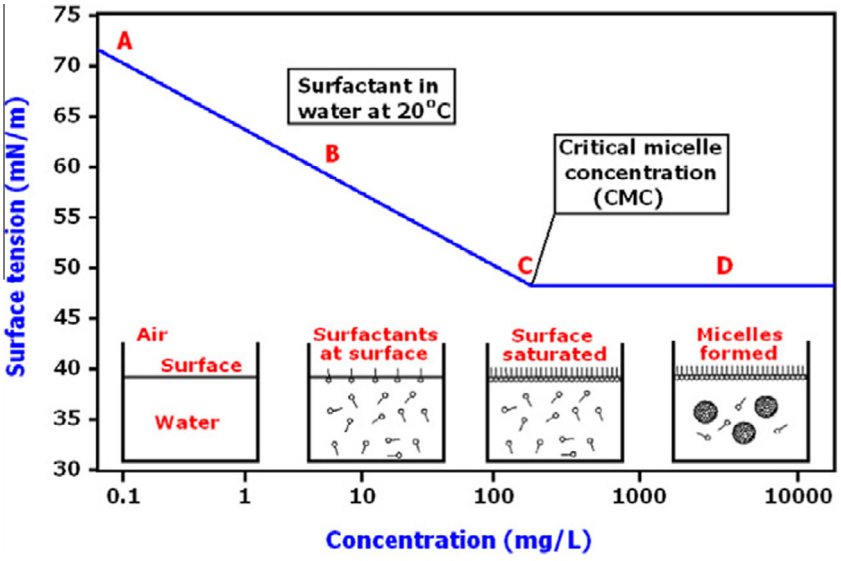


**Figure 3** Schematic representation for adsorption process of surfactant molecules on carbon steel surface: (A) at zero concentration of the inhibitor, (B) before CMC, (C) at CMC, (D) after CMC.

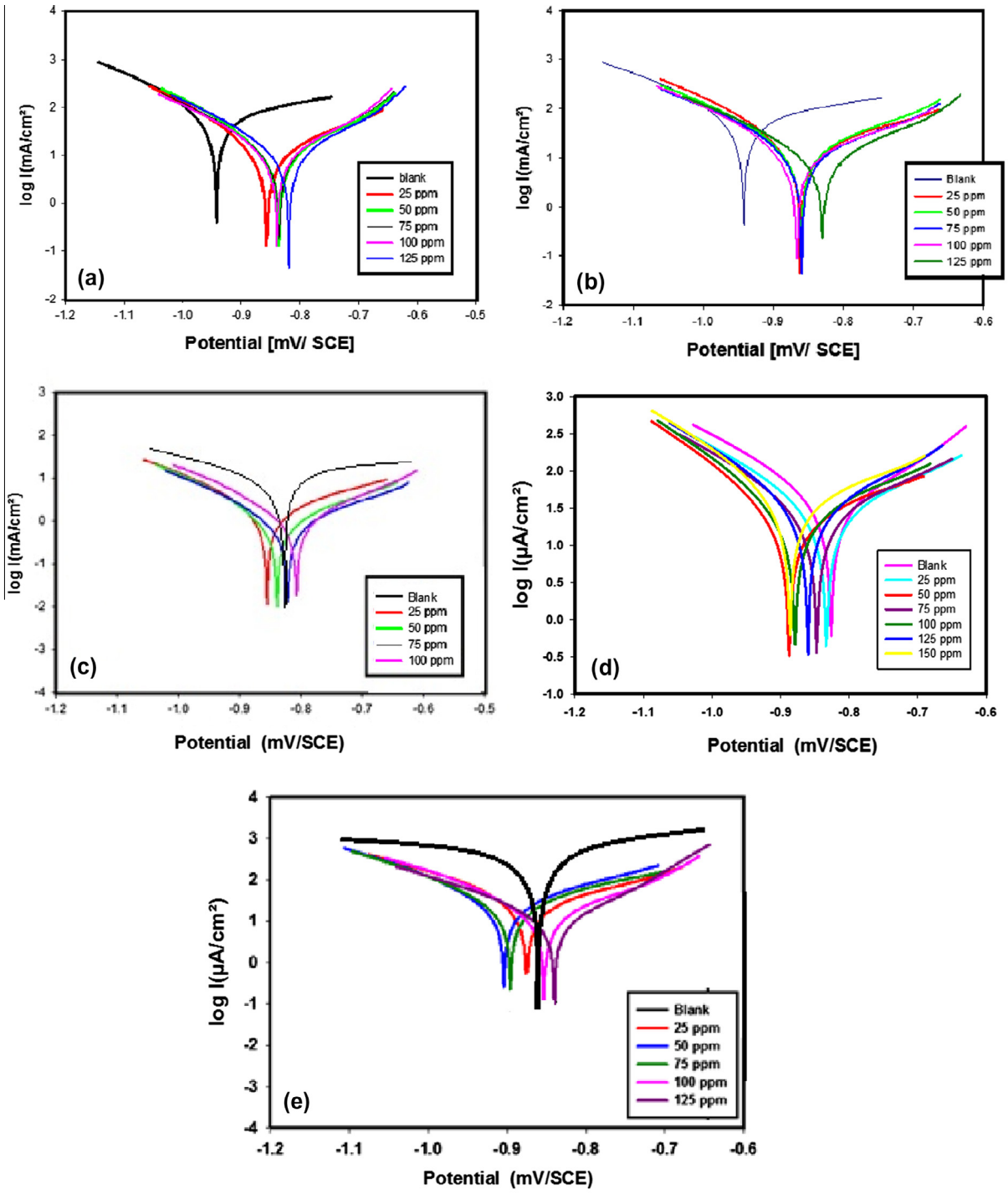


**Figure 4** Potentiodynamic polarization curves ($E$–log I relationship) of carbon steel in formation water in the absence and presence of different concentrations of inhibitors (a) [$DABE_{100}$ (b) $DAHE_{100}$ (c) $DAOE_{100}$ (d) $DAOE_{50}$ and (e) $DAOE_{150}$].

greater than $DAOE_{100}$ and DAOE50 in inhibition efficiency, and this is due to as ethylene oxide increases the solubility of molecule increase, and then the adsorption on the surface metal increases, so the efficiency increases.

Hence, the order of increasing inhibition efficiency is as follows: $DABE_{100} > DAHE_{100}, > DAOE_{100}$ with values 88.2 > 86.9 > 83.9% respectively. This is clear in Table 4. Moreover, as the number of internal alkyl chains decreases, the corrosion inhibition efficiency increases significantly, and also as the number of ethylene oxide increases, the inhibition efficiency increases.

### 3.2. Surface activity and thermodynamic properties

The CMC values of the synthesized surfactants were determined at 298 K from the change in the slope of the plotted

**Table 5** Electrochemical polarization parameters for the corrosion of carbon steel in formation water containing various concentrations of the investigated inhibitors.

| Inhibitor Blank | Concentration, ppm<br>0 | $-E_{corr}$, mV vs. SCE<br>940.8 | $I_{corr}$, mA cm$^{-2}$<br>103.0 | $\beta_a$, mV dec$^{-1}$<br>800.1 | $-\beta_c$, mV dec$^{-1}$<br>202 | $\eta_p$, % |
|---|---|---|---|---|---|---|
| DABE-$_{100e.o}$ | 25 | 861.7 | 70.3 | 308.7 | 163.3 | 31.75 |
| | 50 | 860.6 | 68.4 | 253.2 | 168.3 | 33.59 |
| | 75 | 859.6 | 63.6 | 254 | 152.1 | 38.25 |
| | 100 | 838.9 | 55.6 | 243.7 | 182.8 | 46.02 |
| | 125 | 829.4 | 53.5 | 193.7 | 168.2 | 48.06 |
| DAHE-$_{100e.o}$ | 25 | 856 | 71.6 | 377.1 | 164.5 | 30.49 |
| | 50 | 835.8 | 70.7 | 270.6 | 172.9 | 31.36 |
| | 75 | 851 | 69.6 | 307.9 | 175 | 32.43 |
| | 100 | 838.2 | 64.1 | 223 | 177.9 | 37.77 |
| | 125 | 819.2 | 60.2 | 237 | 179.2 | 41.55 |
| DAOE-$_{100e.o}$ | 25 | 858.2 | 73.8 | 318.7 | 183.8 | 28.35 |
| | 50 | 833.4 | 71.5 | 188.6 | 178.4 | 30.58 |
| | 75 | 838.2 | 68.64 | 205.3 | 165.3 | 33.36 |
| | 100 | 824.2 | 65.7 | 256.6 | 173.5 | 36.21 |
| | 125 | 811.3 | 62.6 | 163.4 | 144.7 | 39.22 |

data of surface tension (c) versus the natural logarithm of the solute molar concentration; ln C, as shown in Fig. 2. The critical micelle concentration (CMC) is the point of concentration at which it becomes thermodynamically favorable for surfactant molecules in solution to form aggregates (micelles) in order to minimize interaction of either their head groups or their tail groups with the solvent. For the investigation under poly ethoxylated non-ionic surfactant molecules in water, mobilization is due to entropy considerations. Water molecules in close proximity to the hydrophobic group of the surfactant molecules take on a certain ordered configuration, which is entropically unfavorable. Once the surfactant concentration reaches a certain value (CMC), the water structure forces aggregation of the hydrophobic tail groups forming surfactant micelles as illustrated in the schematic diagram Fig. 3. Surface tension plots indicate that each surfactant is molecularly dispersed at low concentration, leading to a reduction in surface tension until certain concentration is reached the surfactant molecules form micelles, which are in equilibrium with the free surfactant molecules as shown in Fig. 2 for $DABE_{100}$, $DAHE_{100}$ and $DAOE_{100}$. The CMC values of the inhibitors were calculated from the abrupt change in the slope of ($\gamma$) against (ln C). The surface active properties of the prepared inhibitors, effectiveness of surface tension reduction ($\pi_{cmc}$), surface excess concentration ($\Gamma_{max}$), minimum surface area per molecule ($A_{min}$), Gibbs free energy of micellization ($\Delta G_{mic}$) and Gibbs free energy of adsorption ($\Delta G_{ads}$) were calculated from the following equations.

$$\pi_{cmc} = \gamma_o - \gamma_{cmc} \quad (1)$$

where $\gamma_o$ is the surface tension measured in pure water at the appropriate temperature and $\gamma_{cmc}$ is the surface tension at CMC.

$$\Gamma_{max} = -[1/RT][d\gamma/d\mathrm{Ln}C]T \quad (2)$$

where ($\Gamma$) is called surface excess concentration of surfactant (mol/cm$^3$), $R$ is the gas constant ($R$ = 8.314 J/mol K), $T$ is the temperature in K, $\gamma$ is the surface or interfacial tension (mN/m) and $C$ is the concentration of surfactant (mol/L).

$$A_{min} = 10^{16}/[\Gamma_{max} \cdot NA] \quad (3)$$

where $A_{min}$ is the surface area per molecule of solute in square nanometres (nm$^2$), $\Gamma$ is the surface excess in mol/m$^2$ and $NA$ is Avogadro's number.

$$\Delta G_{mic} = RT(1+\alpha)\mathrm{LnCMC} \quad (4)$$

where $R$ is the gas constant, $T$, absolute temperature, and $\alpha$ is the fraction of counter ions bound by the micelle in case of ionic surfactants ($\alpha$ = 0 for non-ionic surfactant)

$$\Delta G_{ads} = \Delta G_{mic} - [0.6022 \times \pi_{CMC} \times A_{min}] \quad (5)$$

By careful inspection of the values of CMC, it can be concluded that CMC values increase as the number of ethylene oxide units increases. It is clear that as the surfactant with larger ethylene oxide units is more hydrophilic, hence a larger concentration of them in solution is necessary for micelle formation to become thermodynamically favorable. The data of surface activity and thermodynamic parameters of the prepared inhibitors are tabulated in (Table 3). The results of the thermodynamic parameters of micellization expressed by the standard Gibbs free energy, $\Delta G_{mic}$, (micellization) and $\Delta G_{ads}$ (adsorption) of the inhibitors are listed in (Table 3). Since ($\Delta G_{mic} < 0$), then mobilization has been a spontaneous process, and in addition, the $\Delta G_{ads}$ negative values are greater than $\Delta G_{mic}$, indicating that the inhibitors preferred to adsorb on the interface than to form micelles. Since adsorption on the interface is associated with a decrease in the free energy of the system, then there is a direct relationship between the efficiency of inhibitors and the values of $\Delta G_{ads}$.

### 3.3. Potentiodynamic polarization measurements

Polarization measurements were carried out in order to gain knowledge concerning the kinetics of the cathodic and anodic reactions.Fig. 4(a–e) shows the cathodic and anodic polarization curves of carbon steel immersed in deep oil wells formation water in the absence and presence of different concentrations of the inhibitors. Electrochemical parameters

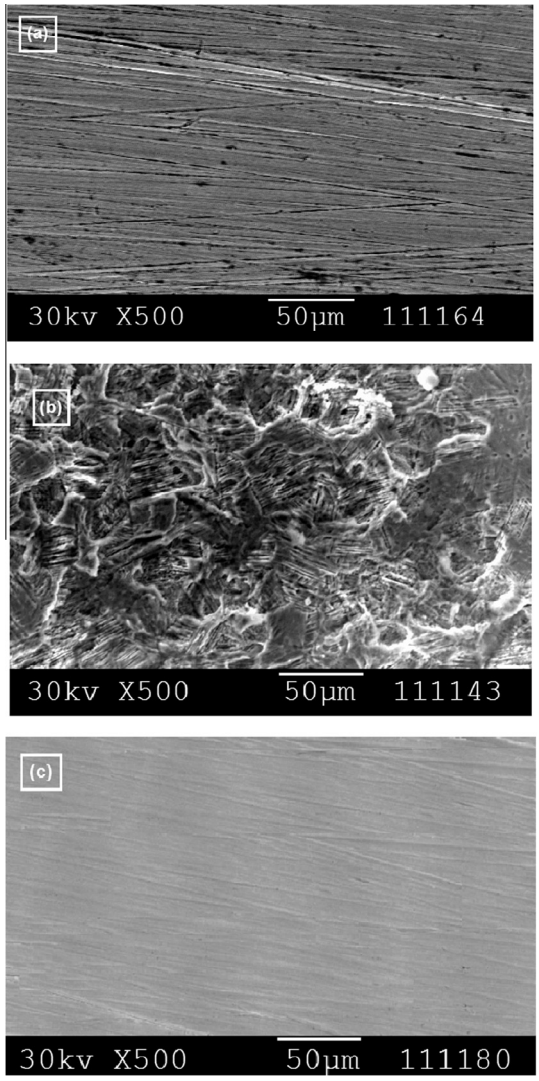


**Figure 5** SEM images for the carbon steel surface: (a) polished sample, (b) after immersion in the oil wells formation water and (c) after immersion in the oil wells formation water in the presence of 125 ppm of inhibitor ($DABE_{100}$).

such as corrosion potential (Ecorr), corrosion current density (icorr), cathodic and anodic Tafel slopes (bc and ba) were calculated. From the obtained polarization curves, it is clear that the corrosion current densities (icorr) were decreased with increasing concentration of inhibitors with respect to the blank (inhibitor free solution). These results confirm the formation of a good protective layer on the surface of carbon steel. The degree of surface coverage (θ) and the percentage inhibition efficiency (η%) were calculated using the following equations [24]:

$$\theta = 1 - I/I_o \quad (6)$$

$$\eta\ (\%) = (1 - I/I_o) \times 100 \quad (7)$$

where $I_o$ and $I$ are the corrosion current densities in the absence and presence of the inhibitor, respectively.

From the obtained data, it is clear that Tafel lines are shifted to more negative and more positive potentials for the anodic and cathodic processes, respectively relative to the blank curve. This means that the selected compound acts as a mixed type inhibitors, i.e., promoting retardation of both anodic and cathodic discharge reactions. The values of cathodic Tafel slope ($b_c$) and anodic Tafel slope ($b_a$) of the inhibitors are found to change with inhibitor concentration, indicating that the inhibitor controlled both the reactions. In other words, the inhibitors decrease the surface area for corrosion without affecting the mechanism of corrosion and only cause inactivation of a part of the surface with respect to the corrosive medium [25]. Complete data obtained from polarization measurements are summarized and listed in Table 4. The results indicate the percentage inhibition efficiency ($\eta$%) of the inhibitor ($DABE_{100}$) is greater than that of inhibitors ($DAHE_{100}$ and $DAOE_{100}$), this could be due to the decrease in length of internal alkyl chain, and also ($\eta$%) of ($DAOE_{150}$) is greater than that of ($DAOE_{100}$) and ($DAOE_{50}$), this could be attributed to the increase in the number of ethylene oxide units of inhibitor molecules, which promotes stronger adsorbed film and hence more protective layer and higher inhibition efficiency. Also, it noticed that the corrosion inhibition enhances with increasing the inhibitor concentration. This behavior is due to the fact that the adsorption amount and coverage of inhibitor on carbon steel surface increases with the inhibitor concentrations [26]. Table 5 shows the inhibition efficiency of the starting amines, and it's clear from this table that the 1,4 DAB exhibited higher efficiency 48.05% relative to 41.55 and 39.22% in 1,6 DAH and 1,8 DAO respectively. This behavior is due to the difference in the number of internal alkyl chains, but in comparison with the data in Table 4, after ethoxylation we can find that the increases in the number of ethylene oxide units of inhibitor molecules increase the inhibition efficiency of inhibitors.

**Table 6** Quantum chemical parameters of the investigated inhibitor.

| Inhibitor | $E_{HOMO}$ (eV) | $E_{LUMO}$ (eV) | $\Delta E$ (eV) | $\mu$ (debye) | I.E. % |
|---|---|---|---|---|---|
| DAB | −7.97 | 3.26 | 11.23 | 1.26 | 45 |
| $DABE_{100}$ | −8.54 | 0.345 | 8.88 | 0.935 | 85 |
| DAH | −9.17 | 2.29 | 11.46 | 2.105 | 40 |
| $DAHE_{100}$ | −8.52 | 1.67 | 10.19 | 0.96 | 82 |
| DAO | −9.66 | 2.31 | 11.97 | 2.104 | 38 |
| $DAOE_{100}$ | −8.51 | 2.49 | 11.00 | 0.97 | 78 |

### 3.4. Scanning electron microscopy (SEM)

Fig. 5a shows an SEM image of polished carbon steel surface. Fig. 5b shows SEM of the surface of carbon steel specimen after immersion in formation water for 60 days in the absence of inhibitor, while Fig. 5c shows SEM of the surface of another carbon steel specimen after immersion in formation water for the same time interval in the presence of 125 ppm of the inhibitor $DABE_{100}$. The resulting scanning electron micrographs reveal that, the surface was strongly damaged in the absence of the inhibitor, but in the presence of 125 ppm of the inhibitor $DABE_{100}$, there is less damage on the surface. This confirms the observed high inhibition efficiency of the inhibitor $DABE_{100}$ at this concentration.

Please cite this article in press as: A.M. Al-Sabagh et al., Synthesis of non-ionic surfactants based on alkylene diamine and evaluation of their corrosion inhibition efficiency on carbon steel in formation water, Egypt. J. Petrol. (2016), http://dx.doi.org/10.1016/j.ejpe.2016.03.001

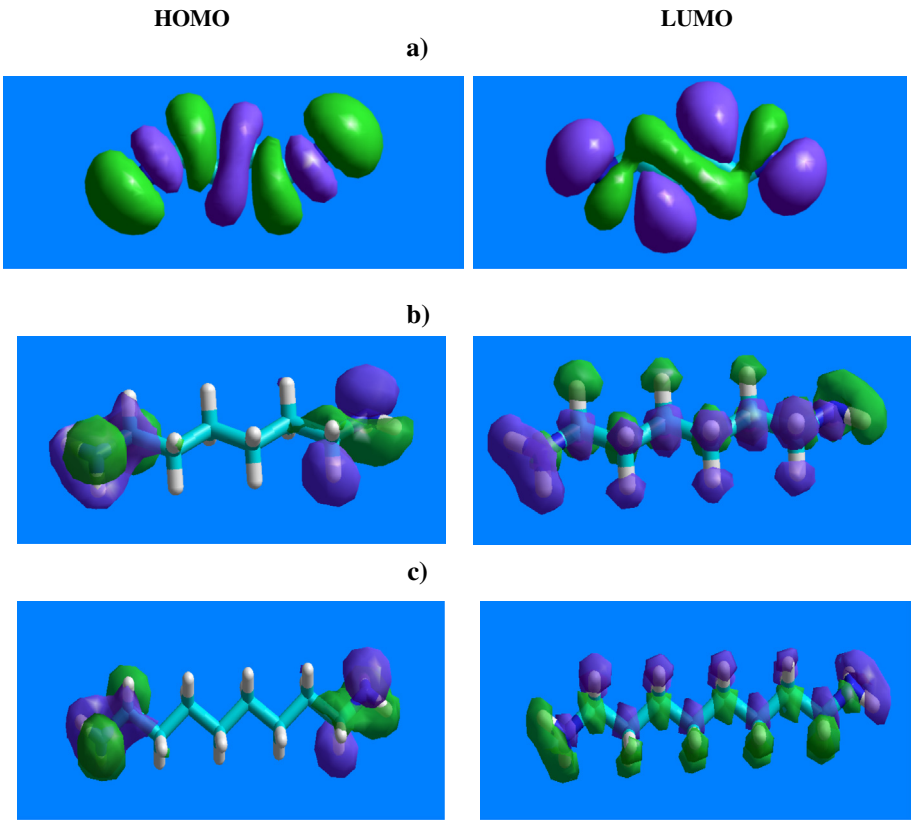


**Figure 6** The frontier molecule orbital density distributions of (a) DAB (b) DAH (c) DAO.

### 3.5. Quantum chemical study

The effectiveness of an inhibitor can be related to its spatial molecular structure, as well as with their molecular electronic structure. The quantum chemical method is introduced to study the relationship between the organic molecular structure and the inhibition effect (see Table 5).

Molecular Orbital Energies [($E_{HOMO}$, $E_{LUMO}$, $\Delta E_{LUMO-HOMO}$), eV]: It is well known that $E_{LUMO}$ presented the ability of accepting electrons and $E_{HOMO}$ is associated with the electron donating ability of the molecule. Thus, the lower $E_{LUMO}$, the greater capability of accepting electrons and high $E_{HOMO}$ are likely to indicate a strong tendency of the molecule to donate electrons to appropriate acceptor molecules with low energy, empty electron orbital such as 3d orbital of Fe atom. In the same way low values of the energy gap ($\Delta E = E_{LUMO} - E_{HOMO}$) will render good inhibition efficiencies, because the energy needed to remove an electron from the last occupied orbital will be low [27]. The $\Delta E$ of a molecule is a measure of the hardness or softness of a molecule. Hard molecules are characterized by larger values of $\Delta E$ and vice versa. However, hard molecules are less reactive than soft molecules because the larger the gap between the last occupied orbital and the first virtual orbital for intermolecular electron transfer, the more it is difficult for intermolecular electron transfer to proceed. The presented data in Table 6 show that the ΔE for the non ethoxylated diamines (DAB, DAH and DAO) was 11.23, 11.46 and 11.97 eV, where the value of $\Delta E$ of the ethoxylated same inhibitors was 8.88, 10.19 and 11.0 eV. respectively. This finding means that, the ethoxylated inhibitors are more soft in their adsorption behavior on the steel surface. Furthermore, the electron transfer should become so easy to make more corrosion inhibition. From Fig. 6, the HOMO and LUMO of the studied inhibitors are almost in a plane, implying that HOMO easily donated electrons to the unoccupied 3d-orbital of Fe atoms and meanwhile LUMO also easily accepted electrons from the occupied 4s-orbital of Fe atoms to form binding forces between the inhibitor molecule and Fe atoms on the metal surface. Theoretically, the Fe atom of the carbon steel surface can interact with the inhibitor molecules. The unoccupied 3d-orbit of Fe atom can accept an electron from the HOMO of the inhibitor molecule. On the other hand, 4s-orbital of the Fe atom has the active electrons in the outermost electron shell, which can interact with the LUMO of the inhibitor molecule through the share of the electron cloud. However, the interaction between 4s-orbital of Fe and the LUMO of the inhibitor molecule is weaker than the case between 3d-orbit of Fe atoms and the HOMO of the inhibitor molecule [28].

The quantum chemistry calculation in this study, Table 6, revealed that as the length increases from DAB, DAH and DAO to the ethoxylated $DABE_{100}$, $DAHE_{100}$ and $DAOE_{100}$, the HOMO energy ($E_{HOMO}$) level boosted slightly while the LUMO energy ($E_{LUMO}$) and the energy gap ($\Delta E$) dropped sharply. The linear correlation between the $E_{HOMO}$ energy level and the corrosion inhibition efficiency of the inhibitors proved that the higher the HOMO energy of the inhibitor (less negative values), the greater the trend of offering electrons to the unoccupied d orbital of the metal and the higher the corrosion inhibition efficiency for iron in formation water. In

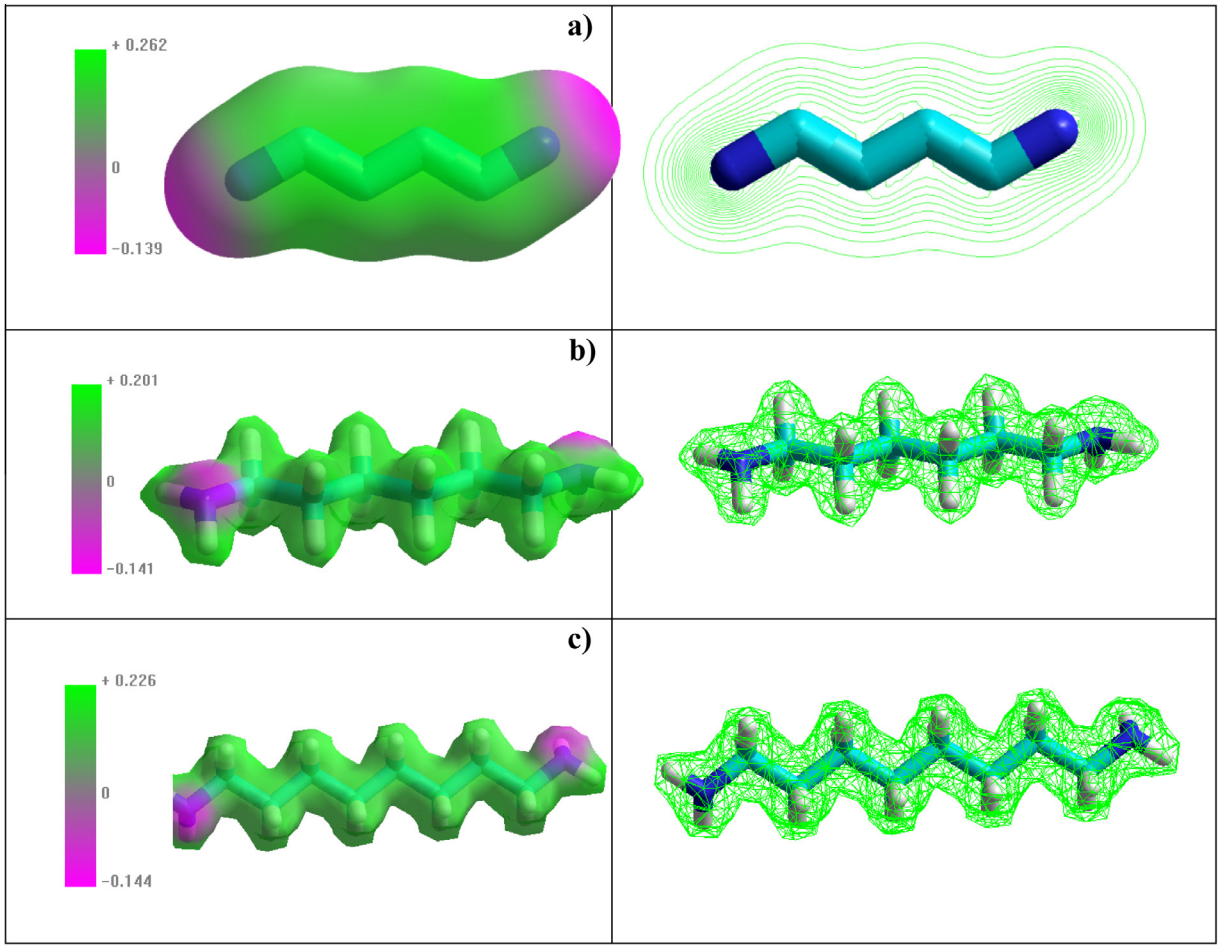


**Figure 7** Molecular electrostatic potential map of the of (a) DAB (b) DAH (c) DAO.

addition, the lower the LUMO energy, the easier the acceptance of electrons from the metal surface. In other words, the inhibition efficiency increases if the compound can donate electrons from its HOMO to the LUMO of the metal, whereby chelation on the metal surface occurs. In addition, as the energy gap ($\Delta E$) decreases, the efficiency of the inhibitors is improved.

With respect the increase of ethylene units the inhibition efficiency increases as shown in Table 4. The space between the two terminal diamine decreases the corrosion inhibition. From the calculated values of the $\Delta E$, the trend for the variation of the inhibition efficiency of the studied inhibitors with decreasing values of $\Delta E$, nearly close to that the deduced from the experimental data "electrochemical measurements".

The inhibition efficiency is sensitive to the changes of the $E_{HOMO}$ and $E_{LUMO}$, which suggested that the inhibitors are perhaps the acceptor or the donor of the electron. This means that, there is electron transferring in the interaction between the inhibitor molecules and both anodic and cathodic sites on the metal surface. Providentially, the $\Delta E$ decreased when the inhibition efficiency increased, which indicates that the inhibitors are more unstable, thus there is the strong interaction between the inhibitors and metal surfaces. The molecular electrostatic potential map of the diamine before ethoxylated is shown in Fig. 7. It is clear from the shown shapes [a, b and c] that electrostatic potentials of 1,4 diamino butane makes a cloud over the molecule to help it adsorb smoothly on the steel surface among the others. By inspecting their inhibition efficiency in Table 5, the 1,4 DAB exhibited theoretical efficiency 45% against 40 and 38% for 1,6 DAH and 1,8 DAO respectively. Fig. 8 shown the HUMO and LUMO of ethoxylated 1,4 DAB, 1,6 DAH and 1,8 DAO at 100 ethylene oxide units. The charge density of nitrogen on the three compounds differs from one to the other, based on the internal alkyl chain length. From these electronic data it can be calculated that the inhibition sufficiency of these inhibitors is depending on the environment of nitrogen grow in the inhibitor molecule and the steric effect of the ethoxylation units, as the results of the 1,4 DAB-$_{100eo}$ exhibited the maximum corrosion inhibition among the 1,6 DAH-$_{100eo}$ or 1,8 DAO-$_{100eo}$.

The dipole moment ($\mu$) is another parameter of the electron distribution in a molecule and is the measure of the polarity of a polar covalent bond. It is related to the hydrophobic character of the molecules [29]. Some authors stated that the inhibition efficiency increases with increasing value of the dipole moment, which depends on the type and nature of molecules considered. However, in most cases, no significant relationship has been found between the dipole moment values and the inhibition efficiency. According to some authors [29] a low value of dipole moment favors the accumulation of inhibitor molecules on the surface, thus increasing the inhibition effectiveness, yet others proposed the opposite correlation, that

Please cite this article in press as: A.M. Al-Sabagh et al., Synthesis of non-ionic surfactants based on alkylene diamine and evaluation of their corrosion inhibition efficiency on carbon steel in formation water, Egypt. J. Petrol. (2016), http://dx.doi.org/10.1016/j.ejpe.2016.03.001

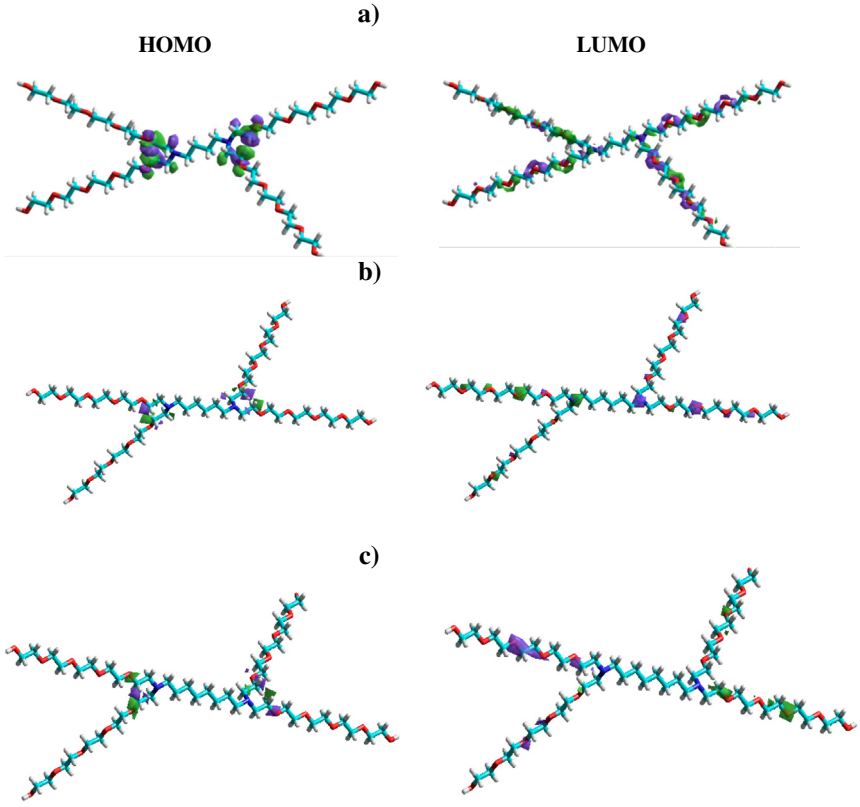


**Figure 8** The frontier molecule orbital density distributions of (a) $DABE_{100}$ (b) $DAHE_{100}$ (c) $DAOE_{100}$.

is, the high dipole moment enhances the adsorption on the metal surface, which in turn contributes to higher inhibition effectiveness. Interestingly, in this study, there is an irregularity appeared in the case of correlation of the dipole moment with the inhibition efficiency. This is clear in Table 6. Since it decreases, the inhibition efficiency increases "inverse relation" upon increasing the monolayer adsorption owing to the size of the molecule became smaller. This observation may be due to the dipole moment, which describes the separation of charge and the geometry of the molecule.

From these electronic data it concluded that the inhibition efficiency of these inhibitors is depending on the environment of nitrogen grown in the inhibitor molecule and the steric effect of the ethoxylation units. As the results of the 1,4 DAB-$_{100E.O}$ exhibited the maximum corrosion inhibitor among the 1,4 DAH-$_{100E.O}$ or 1,8 DAO-$_{100E.O}$.

## 4. Conclusions

All the investigated non-ionic surfactants are effective inhibitors for corrosion of carbon steel in oil wells formation water. The percentage inhibition efficiency (IE%) of the surfactants increases by increasing the degree of ethoxylation of inhibitor molecules.

The potentiodynamic polarization curves indicated that the inhibitor molecules inhibit both anodic metal dissolution and cathodic oxygen reduction, so that the undertaken surfactants classified as mixed – type inhibitors. The critical micelle concentration is considered a key factor in determining the effectiveness of surfactants as corrosion inhibitors due to the large reduction of surface tension at CMC. The inhibition mechanism is attributed to the strong adsorption ability of the selected surfactants on the carbon steel surface, forming a good protective layer, which isolates the surface from the aggressive environment. The relationships between inhibition efficiency of inhibitors and the $E_{HOMO}$, $E_{LUMO}$, the energy gap ($\Delta E$), the dipole moment, log P, and polarizability were calculated using single point ab initio method using Austin model 1. The inhibition efficiency, increased with the increase in $E_{HOMO}$ and the surface area. The polarizability also plays a more important role in the corrosion inhibition course. Increasing polar leads to higher inhibition efficiency. On the other hand, the inhibition efficiency increases with the decrease in $E_{LUMO}$.

## References

[1] F.N. Speller, Corrosion Causes and Prevention, McGraw-Hill, New York, 1951.
[2] B. Rid, T.J. Blakset, D. Queen, Corrosion, NACE, Houston, Texas, 1998, Paper No (78).
[3] O.A. Tomas, P.R. Alan, Production Operations, vol. 2, Oil and Gas Consultants International Inc, Tulsa, 1985.
[4] A.J. McMahon, Colloids Surf. 59 (1991) 187.
[5] J.H. Clint, Surfactant Aggregation, Blackie/Chapman & Hall, Glasgow and London/New York, 1992.
[6] M.M. Osman, A.M.A. Omar, A.M. Sabagh, Mater. Chem. Phys. 50 (1997) 271.
[7] M.A. Migahed, H.M. Mohamed, A.M. Al-Sabagh, Mater. Chem. Phys. 80 (2003) 169.

Please cite this article in press as: A.M. Al-Sabagh et al., Synthesis of non-ionic surfactants based on alkylene diamine and evaluation of their corrosion inhibition efficiency on carbon steel in formation water, Egypt. J. Petrol. (2016), http://dx.doi.org/10.1016/j.ejpe.2016.03.001

[8] F. Hanna, G.M. Sherbini, Y. Brakat, Br. Corros. J. 24 (1989) 269.
[9] M.M. Osman, M.N. Shalaby, Mater. Chem. Phys. 77 (2002) 261.
[10] M.A. Migahed, M. Abd-El-Raouf, A.M. Al-Sabagh, H.M. Abd-El-Bary, Electrochim. Acta 50 (2005) 4683.
[11] A.M. Alsabagh, M.A. Migahed, Hayam S. Awad, Corros. Sci. 48 (2006) 813.
[12] E. Kraka, D. Cremer, J. Am. Chem. Soc. 122 (2000) 8245–8264.
[13] M. Karelson, V. Lobanov, Chem. Rev. 96 (1996) 1027–1043.
[14] A. Hinchliffe, Chemical Modelling From Atoms to Liquids, John Wiley & Sons, New York, 1999.
[15] A. Hinchliffe, Modelling Molecular Structures, John Wiley & Sons, New York, 1994.
[16] M. Bouayed, H. Rabaa, A. Srhiri, J.Y. Saillard, A. Ben Bachir, Corros. Sci. 41 (1999) 501–517.
[17] E. Stupnišek-Lisac, S. Podbršček, T. Sorić, J. Appl. Electrochem. 24 (1994) 779–784.
[18] M.A. Quraishi, R. Sardar, Mater. Chem. Phys. 78 (2002) 425–431.
[19] F. Touhami, A. Aouniti, Y. Abed, B. Hammouti, S. Kertit, A. Ramdani, K. Elkacemi, Corros. Sci. 42 (2000) 929–940.
[20] L. Tang, X. Li, L. Li, G. Mu, G. Liu, Surf. Coat. Technol. 201 (2006) 384–388.
[21] G. Gece, Corros. Sci. 50 (2008) 2981–2992.
[22] E. Ebenso, E. Eno, T. Arslan, K. Kandem, I. Love, C. Retlr, M. S. Lu, S.A. Umoren, Int. J. Quantum Chem. 110 (2010) 2614–2636.
[23] H. Ashassi-Sorkhabi, E. Asghari, Electrochim. Acta 54 (2008) 162.
[24] Q.B. Zhang, Y.X. Hua, Electrochim. Acta 54 (2009) 1881.
[25] Yu.P. Khodyrev, E.S. Batyeva, E.K. Badeeva, E.V. Platova, L. Tiwari, O.G. Sinyashin, Corros. Sci. 53 (2011) 976–983.
[26] M. Al-Sabagh, N.M. Nasser, A.A. Farag, M.A. Migahed, A.M. F. Esau, Egypt. J. Pet. 22 (2013) 101–116.
[27] P.X. Hui, G. Min, Z. YuXuan, W. Qin, H.B. Rong, Sci. China Ser. B: Chem. (2011) 4332–4339.
[28] N. Khalil, Electrochim. Acta 48 (2003) 2635–2640.
[29] P. Politzer, D.G. Truhlar, Chemical Applications of Atomic and Molecular Electrostatic Potentials, Plenum, New York, 1981.

Please cite this article in press as: A.M. Al-Sabagh et al., Synthesis of non-ionic surfactants based on alkylene diamine and evaluation of their corrosion inhibition efficiency on carbon steel in formation water, Egypt. J. Petrol. (2016), http://dx.doi.org/10.1016/j.ejpe.2016.03.001